Available online at www.sciencedirect.com
ScienceDirect
Journal of Sound and Vibration 320 (2009) 632–648
JOURNAL OF SOUND AND VIBRATION
www.elsevier.com/locate/jsvi

Prediction capabilities of classical and shear deformable beam models excited by a moving mass

Keivan Kiani[a], Ali Nikkhoo[a,*], Bahman Mehri[b]

[a]Department of Civil Engineering, Sharif University of Technology, P.O. Box 11365-9313 Tehran, Iran
[b]Department of Mathematical Sciences, Sharif University of Technology, Tehran, Iran

Received 2 March 2008; received in revised form 28 July 2008; accepted 7 August 2008
Handling Editor: A.V. Metrikine.
Available online 5 October 2008

Abstract

In this paper, a comprehensive assessment of design parameters for various beam theories subjected to a moving mass is investigated under different boundary conditions. The design parameters are adopted as the maximum dynamic deflection and bending moment of the beam. To this end, discrete equations of motion for classical Euler–Bernoulli, Timoshenko and higher-order beams under a moving mass are derived based on Hamilton's principle. The reproducing kernel particle method (RKPM) and extended Newmark-β method are utilized for spatial and time discretization of the problem, correspondingly. The design parameter spectra in terms of the beam slenderness, mass weight and velocity of the moving mass are introduced for the mentioned beam theories as well as various boundary conditions. The results indicate the existence of a critical beam slenderness mostly as a function of beam boundary condition, in which, for slenderness lower than this so-called critical one, the application of Euler–Bernoulli or even Timoshenko beam theories would underestimate the real dynamic response of the system. Moreover, there would be a roughly linear relation between the weight of the moving mass and the design parameters for a certain value of the moving mass velocity in most cases of boundary conditions.

1. Introduction

Dynamics of beam structures subjected to moving loads has been investigated for over a century. The importance of such a problem arises in the structural design of bridges in which the nature of loading could affect the design parameters substantially. On the other hand, the inertial effects of moving loads through the dynamic behavior of beams cannot be disregarded as long as the mass weight of the moving load is relatively large compared to the mass of the main structure, e.g. [1–6]. A comprehensive literature survey on the dynamic behavior of solids under moving loads and moving masses has been provided by Frýba [7]. According to his book, based on the complexities induced by consideration of moving mass inertia in problem formulation and solution, in the majority of cases, the effect of mass inertia has been dropped in problem formulation.

*Corresponding author.
E-mail addresses: k_kiani@civil.sharif.ir (K. Kiani), nikkhoo@civil.sharif.ir (A. Nikkhoo), mehri@sharif.ir (B. Mehri).

0022-460X/$ - see front matter © 2008 Elsevier Ltd. All rights reserved.
doi:10.1016/j.jsv.2008.08.010

Ting et al. [8] developed a general algorithm to examine the dynamic response of a finite elastic Euler–Bernoulli beam (EB) supporting a moving mass. Their results (time history of midspan deflection) were in good agreement with those of experiments for a uniform simply supported beam and different velocities of the moving mass. Esmailzadeh and Ghorashi [9] scrutinized the vibration of an EB traversed by a uniform partially distributed moving mass. They stated that the proposed approach could well be applied to the beams with different boundary conditions. Moreover, the length of the distributed moving mass was reported as a crucial parameter which affects the dynamic behavior of the beam remarkably. A comprehensive parametric study on the effects of moving mass weight and velocity on the dynamic behavior of a simply supported EB was done by Nikkhoo et al. [10], employing the eigenfunction expansion method. They introduced a concept of critical velocity in terms of beam fundamental period and span as well as the moving mass weight in which the effect of convective accelerations in moving mass formulation was no more negligible for masses moving with velocities greater than this critical one. Lee [11] found that the interaction force between the mass and the beam depends on both the velocity of the moving mass and the flexibility of the beam. He monitored the onset of separation between the mass and EB by checking the contact force between the moving mass and the beam during the excitation. This phenomenon was demonstrated to have unnegligible effects on the dynamic response of the beam as the mass ratio of the moving mass increases, especially at a high velocity of moving mass.

For the case of a moving mass along a Timoshenko beam (TB), Makertich [12] investigated the response of a simply supported TB and compared the results with the response of an appropriate EB. His proposed method is not easily pertinent to other boundary conditions. Lee [13] studied the dynamic response of a TB acted upon by a moving mass using the Lagrangian approach and the assumed mode method. He verified the results of the model with those of an equivalent moving load for mid-span deflection of a simply supported beam for a few number of moving mass weights and velocities as well as different slenderness ratios of the base beam. Yavari et al. [14] analyzed the dynamic response of TB under a moving mass based on the discrete element technique. They studied the effects of beam slenderness and moving mass velocities for different boundary conditions of the beam. Lou et al. [15] presented a finite element formulation of a TB subjected to a moving mass. Their results were in good agreement with those obtained using the assumed mode method employed by Lee [13].

According to the literature, analytical solutions for the problem of beams subjected to a moving mass are possible only in relatively few special cases; therefore, employing effective numerical methods would be of interest to overcome the limitations of analytical methods. To this end, the reproducing kernel particle method (RKPM) is applied to different beam theories under moving mass excitation. For the first time, RKPM was proposed by Liu et al. [16,17] for structural dynamic analysis. This new method was established to improve the accuracy of the smooth particle hydrodynamics (SPH) method for finite domain problems. In this method, the kernel function is modified by introducing a correction to meet the reproducing conditions. The resulting modified kernel function exactly reproduces polynomials to a specified order and thereby satisfies the completeness conditions [18]. Application of the RKPM to elastic and elastic–plastic one-dimensional (1D) bar problems for both small and large deformations as well as two-dimensional (2D) ones shows remarkable results compared to the results of the finite element method [17].

In this work, an evaluation of design parameters for various beam theories, subjected to a moving mass under different boundary conditions, is scrutinized in some detail. In this regard, the maximum deflection (serviceability criteria) and maximum bending moment (strength criteria) of the beam are considered as the important design parameters. Furthermore, other design criteria, such as maximum slope at supports or maximum shear force, could be taken into account. However, in this study the major focus is on the determination of beams maximum deflection and bending moment. By employing Hamilton's principle, discrete equations of motion of EB, TB and higher-order beams (HOB) under a moving mass are derived. RKPM is utilized for spatial discretization, and an extension of the well-known Newmark-β method is employed for the proper time discretization of the problem. According to the best of the authors knowledge, the effects of beam slenderness, mass weight and velocity of the moving mass on the design parameters have not been addressed for the mentioned beam theories, under various boundary conditions. To this end, nondimensional spectra are introduced dealing with the design parameters for different beam theories. These spectra highlight the effects of beam slenderness through the design parameters for different beam theories and

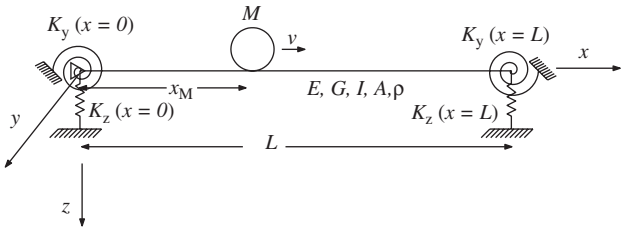

Fig. 1. Schematic single-span elastic beam under a moving mass.

boundary conditions as well as the effects of mass weight and velocity of the moving mass. The results show the existence of a critical slenderness mostly as a function of the beam boundary condition, in which for slenderness lower than this so-called critical one, the application of Euler–Bernoulli or even Timoshenko beam theories could not predict the real dynamic response of the system properly. Furthermore, except for a cantilever beam, there exists a roughly linear relation between the weight of moving mass and design parameters for a specific velocity of the moving mass.

2. Definition of the problem

Consider a finite beam traversed by a moving mass of mass M having a constant velocity of v along the beam as shown in Fig. 1. The beam is axially fixed in one end and connected to the axial and rotary springs at both ends with constants K_z and K_y, respectively. A coordinate system xyz is assumed to be fixed to the left-hand end of the undeformed beam, with the x-axis parallel to the longitudinal axis of the beam and the z-axis pointing vertically in the direction of the gravitational acceleration g. Let $u_x(x,z,t)$ and $u_z(x,z,t)$ denote the longitudinal and transverse deformation components of the beam and $\varepsilon_{xx}/\sigma_{xx}$ and γ_{xz}/σ_{xz} represent the normal longitudinal and transverse shear strain/stress components, respectively. The following assumptions are made in the mathematical modeling of the problem. First, the material of the beam is set to be undamped linear isotropic homogeneous with an elastic modulus of E and a shear modulus of G. Second, the beam has a constant cross section with a uniform mass distribution, i.e., the cross-section area, A, and the beam density, ρ, are uniform along the beam. Third, the only applied load is due to moving of the mass on the beam, and both the transverse and the rotary inertia of the beam are considered for dynamic analysis. Fourth, the moving mass travels with a constant velocity in which to be in contact with the beam at all times. Fifth, let $u_z = w(x,t)$; then the transverse acceleration of the mass on the deformed beam is

$$\ddot{w}_M = \left(\frac{\partial^2 w}{\partial t^2} + 2v\frac{\partial^2 w}{\partial x \partial t} + v^2\frac{\partial^2 w}{\partial x^2}\right)_{x=x_M}.$$

On the right-hand side of this equation, the first term represents the vertical acceleration component, the second is the complementary acceleration and the last one stands for the centripetal acceleration [7].

3. Spatial discretization of the problem

The dynamic behavior of the beam is expressed by the Euler–Bernoulli beam theory (EBT), Timoshenko beam theory (TBT) and higher-order beam theory (HOBT). For each theory, the discrete governing equations are derived by applying Hamilton's principle through the use of RKPM for spatial discretization.

3.1. EB formulation

For the transverse motion of the beam, the transverse displacement is considered to be $u_z = w(x,t)$. Based on the EBT, the small rotation of the transverse plane of the beam (the plane which is perpendicular to the x-axis) about the y-axis is equal to $-\partial w/\partial x$ and the longitudinal displacement is given by $u_x = -z\partial w/\partial x$. The small transverse deflection approximation reads $\varepsilon_{xx} = \partial u_x/\partial x = -z\partial^2 w/\partial x^2$, and $\sigma_{xx} = E\varepsilon_{xx}$ is the only nonzero strain and stress components. The total potential energy of the beam and springs system can be

written as

$$\pi = \pi_k - \pi_s + \pi_f, \tag{1}$$

where π_k is the kinematic energy, π_s is the elastic strain energy and π_f is the potential energy of the beam and springs system subjected to the moving mass. These are defined as follows:

$$\begin{aligned}
\pi_k &= \frac{1}{2}\int_\Omega \rho\left[\left(\frac{\partial u_x}{\partial t}\right)^2 + \left(\frac{\partial u_z}{\partial t}\right)^2\right]\mathrm{d}\Omega = \frac{1}{2}\int_0^L \rho\left[A\left(\frac{\partial w}{\partial t}\right)^2 + I\left(\frac{\partial^2 w}{\partial x \partial t}\right)^2\right]\mathrm{d}x,\\
\pi_s &= \frac{1}{2}\int_{\Omega\cup\Gamma_b} \sigma_{xx}\varepsilon_{xx}\,\mathrm{d}\Omega = \frac{1}{2}\int_0^L EI\left(\frac{\partial^2 w}{\partial x^2}\right)^2\mathrm{d}x + \frac{1}{2}\int_{\Gamma_b}\left[K_z w^2 + K_y\left(\frac{\partial w}{\partial x}\right)^2\right]\mathrm{d}\Gamma,\\
\pi_f &= \int_0^L M\left[g - \left(\frac{\partial^2 w}{\partial t^2} + 2v\frac{\partial^2 w}{\partial x \partial t} + v^2\frac{\partial^2 w}{\partial x^2}\right)\right] w\delta(x - x_M)H(L - x_M)\,\mathrm{d}x,
\end{aligned} \tag{2}$$

in which Ω is the beam domain, Γ_b is the beam boundary, δ is the Dirac delta function and I is the second moment inertia of the beam. The theoretical values of the spring constants for various boundary conditions have been presented in Table 1. In Eq. (2), $H(x)$ is the unit step function defined as

$$H(x) = \begin{cases} 0, & x<0,\\ \frac{1}{2}, & x=0,\\ 1, & x>0. \end{cases} \tag{3}$$

The only unknown parameter of the EB problem, $w(x,t)$, could be discretized as $w(x,t) = \sum_{J=1}^{\mathrm{NP}} \phi_J(x) w_J(t)$, where NP is the total number of particles, $\phi_J(x)$ is the RKPM shape function associated with the Jth particle and $w_J(t)$ is the nodal parameter value associated with the Jth particle. Using Hamilton's principle, one obtains

$$\mathbf{M}_b\ddot{\mathbf{w}} + \mathbf{C}_b\dot{\mathbf{w}} + \mathbf{K}_b\mathbf{w} = \mathbf{f}_b, \tag{4}$$

in which

$$\begin{aligned}
[\mathbf{M}_b]_{IJ} &= \int_0^L \rho(A\phi_I\phi_J + I\phi_I'\phi_J')\,\mathrm{d}x + M\phi_I(x_M)\phi_J(x_M)H(L - x_M),\\
[\mathbf{C}_b]_{IJ} &= 2Mv\phi_I(x_M)\phi_J'(x_M)H(L - x_M),\\
[\mathbf{K}_b]_{IJ} &= \int_0^L EI\phi_I''\phi_J''\,\mathrm{d}x + \int_{\Gamma_b}(K_z\phi_I\phi_J + K_y\phi_I'\phi_J')\,\mathrm{d}\Gamma + Mv^2\phi_I(x_M)\phi_J''(x_M)H(L - x_M),\\
[\mathbf{f}_b]_I &= Mg\phi_I(x_M)H(L - x_M),\\
[\mathbf{w}]_J &= w_J(t),
\end{aligned} \tag{5}$$

where $(')$ and $('')$ denote the first and the second derivatives of the function with respect to x, respectively. It should be noted that the only symmetric matrix is $\mathbf{M}_b$, and the asymmetry of other matrices is related to the nonsymmetric effects of the moving mass.

Table 1
The values of K_z and K_y for various boundary conditions

BC[a]	S	C	F
K_z	∞	∞	0
K_y	0	∞	0

[a]BC, S, C and F stand for the boundary condition, simple support, clamped support and free one, respectively.

3.2. TB formulation

Assume $u_z = w(x,t)$ represents the transverse displacement of the beam from the equilibrium state, and the shear displacement of the cross section is taken into account by introducing a new independent variable $\theta = \theta(x,t)$ defined as the deflection angle of the cross section of the beam with respect to the vertical direction. Therefore, the longitudinal displacement at any point of the beam with coordinates (x,z) is expressed as $u_x = -z\theta$. Considering small displacement approximation, one obtains the strain components as $\varepsilon_{xx} = -z\partial\theta/\partial x$ and $\gamma_{xz} = \partial w/\partial x - \theta$ and so, the only nonzero stress field components are $\sigma_{xx} = E\varepsilon_{xx}$ and $\sigma_{xz} = G\gamma_{xz}$. The shear force (Q_T) and the bending moment (M_T) in the beam are given by

$$\begin{aligned} Q_T &= \int_A \sigma_{xz}\,\mathrm{d}A = k' GA\gamma_{xz} = k' GA\left(\frac{\partial w}{\partial x} - \theta\right), \\ M_T &= \int_A \sigma_{xx} z\,\mathrm{d}A = -EI\frac{\partial\theta}{\partial x}, \end{aligned} \tag{6}$$

in which k' is the shear correction factor which is a constant that depends on the cross-section geometry of the beam. Therefore,

$$\begin{aligned} \pi_k &= \frac{1}{2}\int_\Omega \rho\left[\left(\frac{\partial u_x}{\partial t}\right)^2 + \left(\frac{\partial u_z}{\partial t}\right)^2\right]\mathrm{d}\Omega = \frac{1}{2}\int_0^L \rho\left[I\left(\frac{\partial\theta}{\partial t}\right)^2 + A\left(\frac{\partial w}{\partial t}\right)^2\right]\mathrm{d}x, \\ \pi_s &= \frac{1}{2}\int_{\Omega\cup\Gamma_b} (\sigma_{xx}\varepsilon_{xx} + \sigma_{xz}\gamma_{xz})\,\mathrm{d}\Omega \\ &= \frac{1}{2}\int_0^L \left[EI\left(\frac{\partial\theta}{\partial x}\right)^2 + k' GA\left(\frac{\partial w}{\partial x} - \theta\right)^2\right]\mathrm{d}x + \frac{1}{2}\int_{\Gamma_b} \left(K_z w^2 + K_y\theta^2\right)\mathrm{d}\Gamma, \\ \pi_f &= \int_0^L M\left[g - \left(\frac{\partial^2 w}{\partial t^2} + 2v\frac{\partial^2 w}{\partial x\partial t} + v^2\frac{\partial^2 w}{\partial x^2}\right)\right] w\delta(x - x_M)H(L - x_M)\,\mathrm{d}x. \end{aligned} \tag{7}$$

Denoting $w(x,t) = \sum_{J=1}^{\mathrm{NP}} \phi_J(x) w_J(t)$ and $\theta(x,t) = \sum_{J=1}^{\mathrm{NP}} \phi_J(x)\theta_J(t)$, and using Hamilton's principle, one can obtain the following discrete set of equations for the TB under the moving mass after some manipulations:

$$\mathbf{M}_b\ddot{\mathbf{x}} + \mathbf{C}_b\dot{\mathbf{x}} + \mathbf{K}_b\mathbf{x} = \mathbf{f}_b, \tag{8}$$

where

$$\begin{aligned} \mathbf{M}_b &= \begin{bmatrix} \mathbf{M}_b^{ww} & \mathbf{M}_b^{w\theta} \\ \mathbf{M}_b^{\theta w} & \mathbf{M}_b^{\theta\theta} \end{bmatrix}, \quad \mathbf{C}_b = \begin{bmatrix} \mathbf{C}_b^{ww} & \mathbf{C}_b^{w\theta} \\ \mathbf{C}_b^{\theta w} & \mathbf{C}_b^{\theta\theta} \end{bmatrix}, \quad \mathbf{K}_b = \begin{bmatrix} \mathbf{K}_b^{ww} & \mathbf{K}_b^{w\theta} \\ \mathbf{K}_b^{\theta w} & \mathbf{K}_b^{\theta\theta} \end{bmatrix}, \\ \mathbf{f}_b &= \begin{Bmatrix} \mathbf{f}_b^{w} \\ \mathbf{f}_b^{\theta} \end{Bmatrix}, \quad [\mathbf{x}]_J = \begin{Bmatrix} w_J(t) \\ \theta_J(t) \end{Bmatrix}, \end{aligned} \tag{9}$$

in which the appropriate nonzero submatrices are defined as

$$\begin{aligned} [\mathbf{M}_b^{ww}]_{IJ} &= \int_0^L \rho A\phi_I\phi_J\,\mathrm{d}x + M\phi_I(x_M)\phi_J(x_M)H(L - x_M), \\ [\mathbf{M}_b^{\theta\theta}]_{IJ} &= \int_0^L \rho I\phi_I\phi_J\,\mathrm{d}x, \\ [\mathbf{C}_b^{ww}]_{IJ} &= 2Mv\phi_I(x_M)\phi_J'(x_M)H(L - x_M), \\ [\mathbf{K}_b^{ww}]_{IJ} &= \int_0^L k' GA\phi_I'\phi_J'\,\mathrm{d}x + Mv^2\phi_I(x_M)\phi_J''(x_M)H(L - x_M) + \int_{\Gamma_b} K_z\phi_I\phi_J\,\mathrm{d}\Gamma, \end{aligned}$$

$$[\mathbf{K}_b^{w\theta}]_{IJ} = -\int_0^L k'GA\phi_I'\phi_J\,\mathrm{d}x,$$
$$[\mathbf{K}_b^{\theta w}]_{IJ} = -\int_0^L k'GA\phi_I\phi_J'\,\mathrm{d}x,$$
$$[\mathbf{K}_b^{\theta\theta}]_{IJ} = \int_0^L (k'GA\phi_I\phi_J + EI\phi_I'\phi_J')\,\mathrm{d}x + \int_{\Gamma_b} K_y\phi_I\phi_J\,\mathrm{d}\Gamma,$$
$$[\mathbf{f}_b^{w}]_I = Mg\phi_I(x_M)H(L-x_M). \tag{10}$$

3.3. HOB formulation

In an HOB, the longitudinal displacement is expressed with higher-order functions (third or fifth order) in terms of a variable in the z direction to model shear deformation, but the transverse displacement could be higher order (quadratic or cubic) or constant across the beam thickness [19]. Consider an HOB with a constant transverse deformation across its thickness as $u_z = w(x,t)$, and the longitudinal displacement of the form, $u_x = z\Psi - \alpha z^3(\Psi + \partial w/\partial x)$ [20,21], in which $\alpha = 4/3h^2$ (h is the thickness of the beam) and Ψ is the deflection angle of the cross section of the beam to the reference plane about the y-axis. Therefore, the longitudinal normal and transverse shear components of the strain and stress fields are:

$$\sigma_{xx} = E\varepsilon_{xx};\quad \varepsilon_{xx} = z\frac{\partial\Psi}{\partial x} - \alpha z^3\left(\frac{\partial\Psi}{\partial x} + \frac{\partial^2 w}{\partial x^2}\right),$$
$$\sigma_{xz} = G\gamma_{xz};\quad \gamma_{xz} = (1-3\alpha z^2)\left(\Psi + \frac{\partial w}{\partial x}\right). \tag{11}$$

The transverse shear stress defined in Eq. (11) satisfies the traction-free condition on the top and the bottom surfaces of the beam. The shear force and the bending moment in the beam are given by

$$Q_H = \kappa\left(\Psi + \frac{\partial w}{\partial x}\right),$$
$$M_H = J_2\frac{\partial\Psi}{\partial x} - \alpha J_4\left(\frac{\partial\Psi}{\partial x} + \frac{\partial^2 w}{\partial x^2}\right), \tag{12}$$

in which

$$\kappa = \int_A G(1-3\alpha z^2)\,\mathrm{d}A, \tag{13}$$

$$J_n = \int_A Ez^n\,\mathrm{d}A;\quad n = 2,4,6. \tag{14}$$

The parameters π_k, π_s and π_f for the HOB under the moving mass take the following form:

$$\pi_k = \frac{1}{2}\int_0^L [I_0\dot{w}'^2 + I_2\dot{\Psi}^2 - 2\alpha I_4\dot{\Psi}(\dot{\Psi}+\dot{w}') + \alpha^2 I_6(\dot{\Psi}+\dot{w}')^2]\,\mathrm{d}x,$$
$$\pi_s = \frac{1}{2}\int_0^L [J_2\Psi'^2 - 2\alpha J_4\Psi'(\Psi'+w'') + \kappa(\Psi+w')^2 + \alpha^2 J_6(\Psi'+w'')^2]\,\mathrm{d}x + \frac{1}{2}\int_{\Gamma_b}(K_z w^2 + K_y\Psi^2)\,\mathrm{d}\Gamma,$$
$$\pi_f = \int_0^L M[g - (\ddot{w} + 2v\dot{w}' + v^2 w'')]w(x,t)\delta(x-x_M)H(L-x_M)\,\mathrm{d}x, \tag{15}$$

where $I_n = \int_A \rho z^n\,\mathrm{d}A$. Denoting $w(x,t) = \sum_{J=1}^{\mathrm{NP}}\phi_J(x)w_J(t)$ and $\Psi(x,t) = \sum_{J=1}^{\mathrm{NP}}\phi_J(x)\Psi_J(t)$, and utilizing the Hamilton's principle, leads to the equations of motion as

$$\mathbf{M}_b\ddot{\mathbf{x}} + \mathbf{C}_b\dot{\mathbf{x}} + \mathbf{K}_b\mathbf{x} = \mathbf{f}_b, \tag{16}$$

in which

$$\mathbf{M}_b=\begin{bmatrix}\mathbf{M}_b^{ww} & \mathbf{M}_b^{w\Psi}\\ \mathbf{M}_b^{\Psi w} & \mathbf{M}_b^{\Psi\Psi}\end{bmatrix},\quad \mathbf{C}_b=\begin{bmatrix}\mathbf{C}_b^{ww} & \mathbf{C}_b^{w\Psi}\\ \mathbf{C}_b^{\Psi w} & \mathbf{C}_b^{\Psi\Psi}\end{bmatrix},\quad \mathbf{K}_b=\begin{bmatrix}\mathbf{K}_b^{ww} & \mathbf{K}_b^{w\Psi}\\ \mathbf{K}_b^{\Psi w} & \mathbf{K}_b^{\Psi\Psi}\end{bmatrix},$$
$$\mathbf{f}_b=\begin{Bmatrix}\mathbf{f}_b^{w}\\ \mathbf{f}_b^{\Psi}\end{Bmatrix},\quad [\mathbf{x}]_J=\begin{Bmatrix}w_J(t)\\ \Psi_J(t)\end{Bmatrix}, \tag{17}$$

where the appropriate nonzero submatrices are defined as

$$[\mathbf{M}_b^{ww}]_{IJ}=\int_0^L(I_0\phi_I\phi_J+\alpha^2I_6\phi_I''\phi_J'')\,\mathrm{d}x+M\phi_I(x_M)\phi_J(x_M)H(L-x_M),$$
$$[\mathbf{M}_b^{w\Psi}]_{IJ}=\int_0^L(-\alpha I_4\phi_I'\phi_J+\alpha^2I_6\phi_I'\phi_J)\,\mathrm{d}x,$$
$$[\mathbf{M}_b^{\Psi w}]_{IJ}=\int_0^L(-\alpha I_4\phi_I\phi_J'+\alpha^2I_6\phi_I\phi_J')\,\mathrm{d}x,$$
$$[\mathbf{M}_b^{\Psi\Psi}]_{IJ}=\int_0^L(I_2-2\alpha I_4+\alpha^2I_6)\phi_I\phi_J\,\mathrm{d}x,$$
$$[\mathbf{C}_b^{ww}]_{IJ}=2Mv\phi_I(x_M)\phi_J'(x_M)H(L-x_M),$$
$$[\mathbf{K}_b^{ww}]_{IJ}=\int_0^L(\kappa\phi_I'\phi_J'+\alpha^2J_6\phi_I''\phi_J'')\,\mathrm{d}x+\int_{\Gamma_b}K_z\phi_I\phi_J\,\mathrm{d}\Gamma+Mv^2\phi_I(x_M)\phi_J''(x_M)H(L-x_M),$$
$$[\mathbf{K}_b^{w\Psi}]_{IJ}=\int_0^L(-\alpha J_4\phi_I''\phi_J'+\kappa\phi_I'\phi_J+\alpha^2J_6\phi_I''\phi_J')\,\mathrm{d}x,$$
$$[\mathbf{K}_b^{\Psi w}]_{IJ}=\int_0^L(-\alpha J_4\phi_I'\phi_J''+\kappa\phi_I\phi_J'+\alpha^2J_6\phi_I'\phi_J'')\,\mathrm{d}x,$$
$$[\mathbf{K}_b^{\Psi\Psi}]_{IJ}=\int_0^L[(J_2-2\alpha J_4+\alpha^2J_6)\phi_I'\phi_J'+\kappa\phi_I\phi_J]\,\mathrm{d}x+\int_{\Gamma_b}K_y\phi_I\phi_J\,\mathrm{d}\Gamma,$$
$$[\mathbf{f}_b^{w}]_I=Mg\phi_I(x_M)H(L-x_M). \tag{18}$$

4. Time discretization of the problem

In spite of a beam subjected to a moving load, in moving mass problems, the mass matrix, the damping matrix and the stiffness matrix are time dependent as long as the load has not left the beam end. Therefore, use of the Newmark-β method needs some modifications for time discretization which will be explained in some detail. Differentiating both sides of Eq. (16) with respect to the time parameter, t, yields

$$\Delta(\mathbf{M}_b)_i\ddot{\mathbf{x}}_i+(\mathbf{M}_b)_i\,\Delta\ddot{\mathbf{x}}_i+\Delta(\mathbf{C}_b)_i\dot{\mathbf{x}}_i+(\mathbf{C}_b)_i\,\Delta\dot{\mathbf{x}}_i+\Delta(\mathbf{K}_b)_i\mathbf{x}_i+(\mathbf{K}_b)_i\,\Delta\mathbf{x}_i=\Delta\mathbf{f}_i, \tag{19}$$

where $\Delta(\,)_i=(\,)_{i+1}-(\,)_i$ and $(\,)_i$ denotes the value of the parameter $(\,)$ at the time t_i. Using the Newmark-β method [22]

$$\Delta\dot{\mathbf{x}}_i=\Delta t\ddot{\mathbf{x}}_i+\gamma\Delta t\Delta\ddot{\mathbf{x}}_i,$$
$$\Delta\mathbf{x}_i=\Delta t\,\dot{\mathbf{x}}_i+\frac{\Delta t^2}{2}\ddot{\mathbf{x}}_i+\beta\,\Delta t^2\,\Delta\ddot{\mathbf{x}}_i, \tag{20}$$

in which $\Delta t=t_{i+1}-t_i$ and the values of the parameters β and γ are set to be equal to 0.25 and 0.50 in the calculations, respectively. Extracting $\Delta\dot{\mathbf{x}}_i$ and $\Delta\ddot{\mathbf{x}}_i$ in terms of $\Delta\mathbf{x}_i$, $\dot{\mathbf{x}}_i$ and $\ddot{\mathbf{x}}_i$ from Eq. (20) and substituting into Eq. (19) gives

$$\hat{\mathbf{K}}_i\,\Delta\mathbf{x}_i=\Delta\hat{\mathbf{f}}_i, \tag{21}$$

where

$$\hat{\mathbf{K}}_i = \frac{1}{\beta\Delta t^2}(\mathbf{M}_b)_i + \frac{\gamma}{\beta\Delta t}(\mathbf{C}_b)_i + (\mathbf{K}_b)_i,$$
$$\Delta\hat{\mathbf{f}}_i = \Delta\mathbf{f}_i - [\Delta(\mathbf{M}_b)_i\ddot{\mathbf{x}}_i + \Delta(\mathbf{C}_b)_i\dot{\mathbf{x}}_i + \Delta(\mathbf{K}_b)_i\mathbf{x}_i] + \frac{1}{\beta\Delta t}(\mathbf{M}_b)_i\dot{\mathbf{x}}_i + \frac{\gamma}{\beta}(\mathbf{C}_b)_i\dot{\mathbf{x}}_i + \frac{1}{2\beta}(\mathbf{M}_b)_i\ddot{\mathbf{x}}_i - \Delta t\left(1-\frac{\gamma}{2\beta}\right)(\mathbf{C}_b)_i\ddot{\mathbf{x}}_i. \quad (22)$$

The linear set of equations in Eq. (21) could be solved at each time step, and the initial boundary conditions are set for the system to be at rest; i.e., $\mathbf{x}_0 = \mathbf{0}$ and $\dot{\mathbf{x}}_0 = \mathbf{0}$. The values of $\mathbf{x}_{i+1}$, $\dot{\mathbf{x}}_{i+1}$ and $\ddot{\mathbf{x}}_{i+1}$ could be calculated as follows [22]:

$$\mathbf{x}_{i+1} = \mathbf{x}_i + \Delta\mathbf{x}_i,$$
$$\dot{\mathbf{x}}_{i+1} = \dot{\mathbf{x}}_i + \frac{\gamma}{\beta\Delta t}\Delta\mathbf{x}_i - \frac{\gamma}{\beta}\dot{\mathbf{x}}_i + \Delta t\left(1-\frac{\gamma}{2\beta}\right)\ddot{\mathbf{x}}_i,$$
$$\ddot{\mathbf{x}}_{i+1} = \ddot{\mathbf{x}}_i + \frac{1}{\beta\Delta t^2}\Delta\mathbf{x}_i - \frac{1}{\beta\Delta t}\dot{\mathbf{x}}_i - \frac{1}{2\beta}\ddot{\mathbf{x}}_i. \quad (23)$$

5. Parametric studies

A uniform isotropic-homogeneous-prismatic beam is considered. The beam is a single-span one, and its cross section is assumed to be rectangular. In order to study the different parameters affecting the maximum deflection and bending moment of the beam, two normalized parameters $W_{\max,N} = |W_{\max,\mathrm{dyn}}|/W_{\max,\mathrm{st}}$ and $M_{\max,N} = |M_{\max,\mathrm{dyn}}|/M_{\max,\mathrm{st}}$ are considered in which $W_{\max,\mathrm{dyn}}$ and $M_{\max,\mathrm{dyn}}$ denote the maximum dynamic deflection and bending moment along the beam caused by the moving mass, respectively. $W_{\max,\mathrm{st}}$ and $M_{\max,\mathrm{st}}$ are the appropriate maximum static deflection and bending moment along the EB under statically applied force Mg. A proper static analysis would result in $MgL^3/48EI$, $MgL^3/192EI$, $0.0098124MgL^3/EI$ and $MgL^3/3EI$ for $W_{\max,\mathrm{st}}$ according to SS, CC, SC and CF boundary conditions, respectively. Similarly, the appropriate values of $M_{\max,\mathrm{st}}$ based on SS, CC, SC and CF boundary conditions are determined as $MgL/4$, $MgL/8$, $0.174MgL$ and MgL, respectively. Moreover, the nondimensional slenderness, velocity and mass parameters are assumed to be $\lambda = L/r$, $V_N = v/v'$ [10] and $M_N = M/\rho AL$, respectively, where $v' = \pi/L\sqrt{EI/\rho A}$ and r is the gyration radius of the beam cross section according to its neutral axis. The geometrical and material properties of the beam are assumed to be: $L = 10\,(\mathrm{m})$, $E = 2.1\times10^{11}(\mathrm{N\,m^{-2}})$, $G = 8.0769\times10^{10}(\mathrm{N\,m^{-2}})$, $b = 0.1(\mathrm{m})$, $h = \sqrt{12}r$, $k' = 0.833$ and $\rho = 7800(\mathrm{kg\,m^{-3}})$. Moreover, $K_z = 10^4EL(\mathrm{N\,m^{-1}})$ and $K_y = 10^3EL^3(\mathrm{N\,m})$ are considered in the numerical analysis for the case of the undeflected and the unrotated end, respectively. In all of the analysis steps using RKPM, 11 uniformly distributed particles and 5 Gaussian points for each computational cell are considered. Generation of the particle shape functions are fulfilled for a dilation parameter value of 2.5, a linear base function and a third-order spline window function [16]. The shape functions of the RKPM particles, and their first and second derivatives have been presented in Figs. 2(a–c), correspondingly. Besides, the values of the time step are equal to $L/(400v)$ and $L/(200v')$ during the time intervals $0\leqslant t\leqslant L/v$ (first phase) and $t>L/v$ (second phase, i.e., free vibration), respectively.

Through Figs. 3–6, the effects of beam slenderness on the design parameters (maximum dynamic deflection and bending moment of the beam) for different velocities of the moving mass as well as the beam boundary condition are depicted. In all of these figures, the dotted lines represent EB, dashed lines represent TB and solid lines represent HOB. In Figs. 3(a and b), the results are shown for an SS beam. For small values of λ ($\lambda<35$), the results of EB compared to those of shear deformable beams are clearly distinct in which, for the TB and HOB, there exist larger deflections and almost bending moments compared to the results of EB. This distinction becomes more apparent for higher moving mass velocities. Therefore, this assumed slenderness could be nominated as the critical slenderness (λ_{cr}). This would imply that for an SS beam, if its slenderness is higher than λ_{cr}, for any moving mass velocity, the assumptions of EBT lead to a trustable dynamic design of

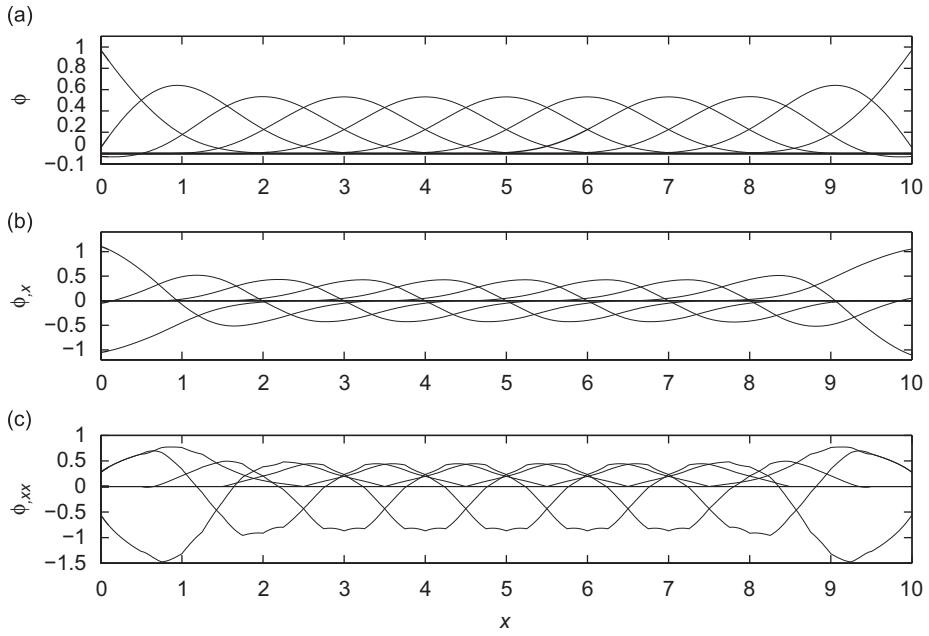

Fig. 2. (a) The RKPM shape functions; (b) first derivative of RKPM shape functions; (c) second derivative of RKPM shape functions.

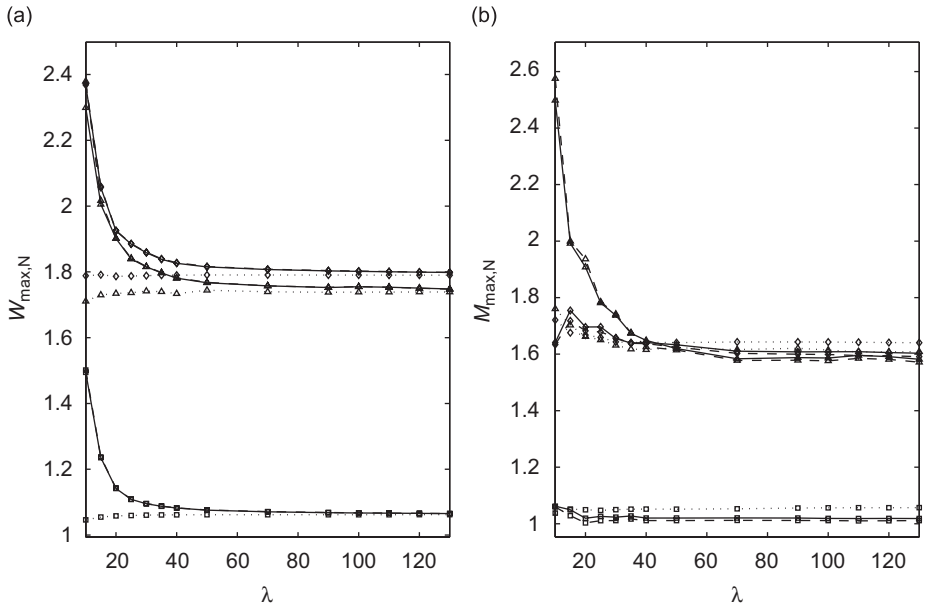

Fig. 3. Effect of beam slenderness on the maximum dynamic response of an SS beam for various values of the moving mass velocity: (a) normalized maximum vertical displacement vs. slenderness; (b) normalized maximum bending moment vs. slenderness ((□)$V_N = 0.1$, (◇)$V_N = 0.5$, (Δ)$V_N = 1.0$; (···) EBT, (−−) TBT, (—) HOBT; $M_N = 0.15$).

beam under the moving mass. Otherwise, the proper use of TBT or HOBT is highly recommended especially for high moving mass velocities. In Fig. 4, the same study is done for a CC beam. According to Fig. 4(a), and for $\lambda > 80$, the maximum deflections of different beam theories show approximately a 5% difference for all moving mass velocities. Moreover, for $\lambda > 80$, the maximum bending moments of EB are greater than those of TB and HOB (see Fig. 4(b)). Thus in this case, $\lambda_{cr} \approx 80$. Similar parametric studies for SC and CF boundary

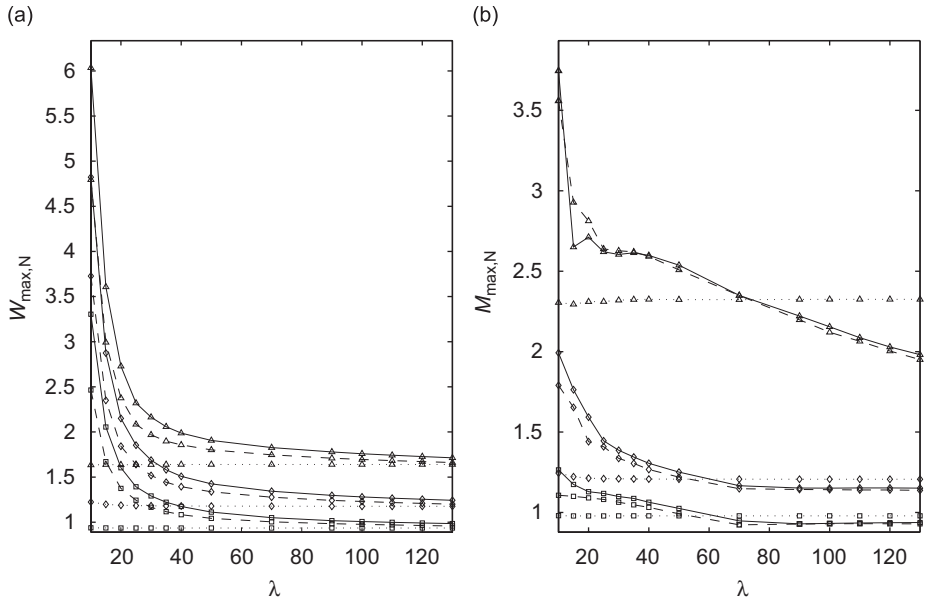

Fig. 4. Effect of beam slenderness on the maximum dynamic response of a CC beam for various values of the moving mass velocity: (a) normalized maximum vertical displacement vs. slenderness; (b) normalized maximum bending moment vs. slenderness ((□)$V_N = 0.1$, (◇)$V_N = 0.5$, (Δ)$V_N = 1.0$; (···) EBT, (−−) TBT, (—) HOBT; $M_N = 0.15$).

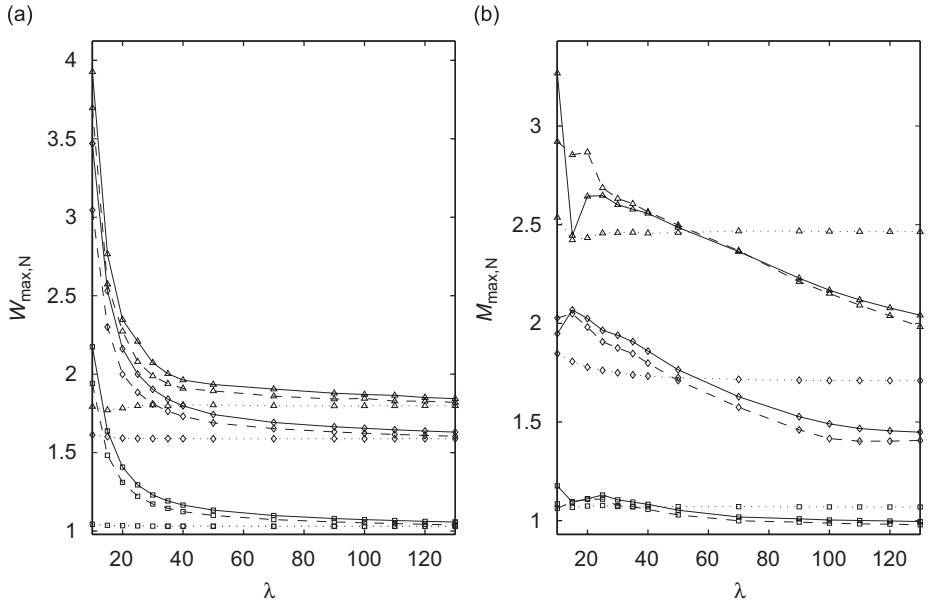

Fig. 5. Effect of beam slenderness on the maximum dynamic response of an SC beam for various values of the moving mass velocity: (a) normalized maximum vertical displacement vs. slenderness; (b) normalized maximum bending moment vs. slenderness ((□)$V_N = 0.1$, (◇)$V_N = 0.5$, (Δ)$V_N = 1.0$; (···) EBT, (−−) TBT, (—) HOBT; $M_N = 0.15$).

conditions are shown in Figs. 5 and 6, respectively. As expected, for the SC beam, the results are somehow between those of the SS and CC, leading to a critical slenderness around 55. A reasonable interpretation is that the magnitude of shear energy of the beam compared to its flexural energy increases as one moves from CF to SS, then SC and finally, CC boundary condition. Therefore the most remarkable differences in the results of

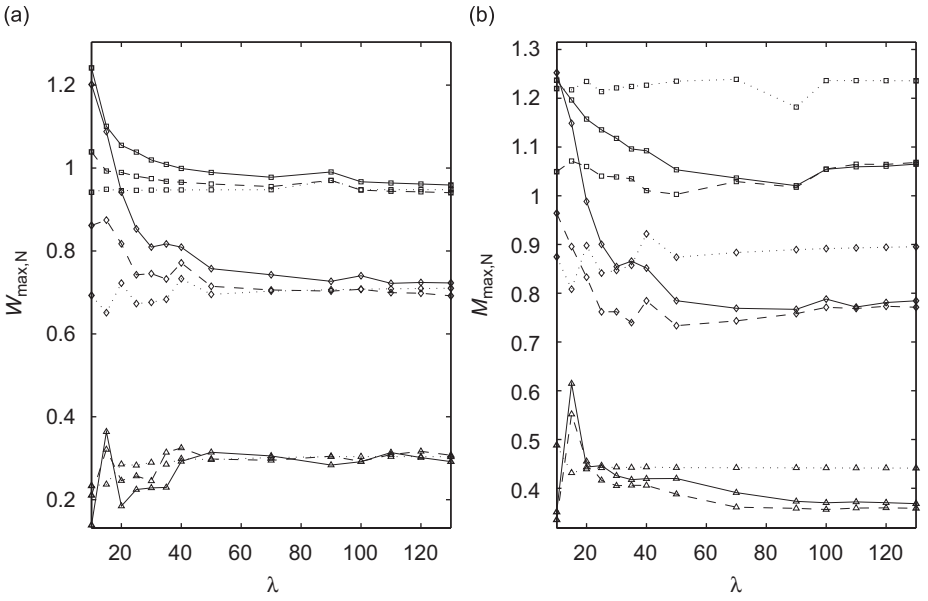

Fig. 6. Effect of beam slenderness on the maximum dynamic response of a CF beam for various values of the moving mass velocity: (a) normalized maximum vertical displacement vs. slenderness; (b) normalized maximum bending moment vs. slenderness; ((□)$V_N = 0.1$, (◇)$V_N = 0.5$, (Δ)$V_N = 1.0$; (···) EBT, (−−) TBT, (—) HOBT; $M_N = 0.15$).

various beam theories, especially for low values of λ, arise in the CC boundary condition, and minimum differences are observed for the CF boundary condition. This can be seen clearly in Figs. 6(a and b), in which there exists a fairly small value as the critical slenderness of the beam.

Another important parametric study could be done on the role of the moving mass velocity for a specified value of beam slenderness regarding different beam theories and boundary conditions. This task is done by plotting deflection and bending moment spectra of the beam in terms of the moving mass velocity as shown in Figs. 7–10. In Fig. 7, the design spectra of an SS beam are shown for different values of λ and assumed beam theory. As Fig. 7(a) shows, for the case of $\lambda = 10$, as expected, the maximum deflection of EB shows a remarkable difference compared with those of TB and HOB for various values of V_N. However, for $V_N < 0.6$, this is not the case for the maximum bending moment of the beam at such a slenderness. As the slenderness of the beam increases, there is no appreciable difference between the results of various beam theories even for high moving mass velocities. The same study for the CC boundary condition is depicted in Fig. 8. Expectedly, for low values of λ and high moving mass velocities, there exists a completely different shape of deflection spectrum for EB compared with those of TB and HOB. This difference is also appreciable in the bending moment spectrum. The increase in λ magnitudes would lessen the differences of design parameter values for all beam theories, especially for low moving mass velocities (say, $V_N < 0.4$). Similarly, the results for SC and CF boundary conditions are shown in Figs. 9 and 10, respectively. As can be seen in Fig. 9, the results of the SC boundary condition are between those of SS and CC boundary conditions to some extent. As Fig. 10 shows, the maximum values of deflection and bending moment for a cantilever beam occur at a fairly lower level of moving mass velocity ($\approx V_N = 0.2$) compared to those of other boundary conditions. Moreover, the effect of beam slenderness on the design parameters, except in very deep beams, is not important at all even for high moving mass velocities. It should be noted that the source of oscillations in Fig. 10 is the separation between the mass and beam, especially for high moving mass velocities, as stated by Lee [11].

For completion of parametric studies, the role of moving mass weight in the design parameters of various beams is investigated. In Figs. 11–14, the maximum deflection and bending moment for different beam boundary conditions due to the change of the mass weight of the moving load is shown. In Figs. 11(c)–14(c), the beam is assumed to be fairly slender as the magnitude of λ is taken to be 120. As discussed earlier, for such a slenderness, the results of different beam theories are close and the use of EBT is substantially acceptable.

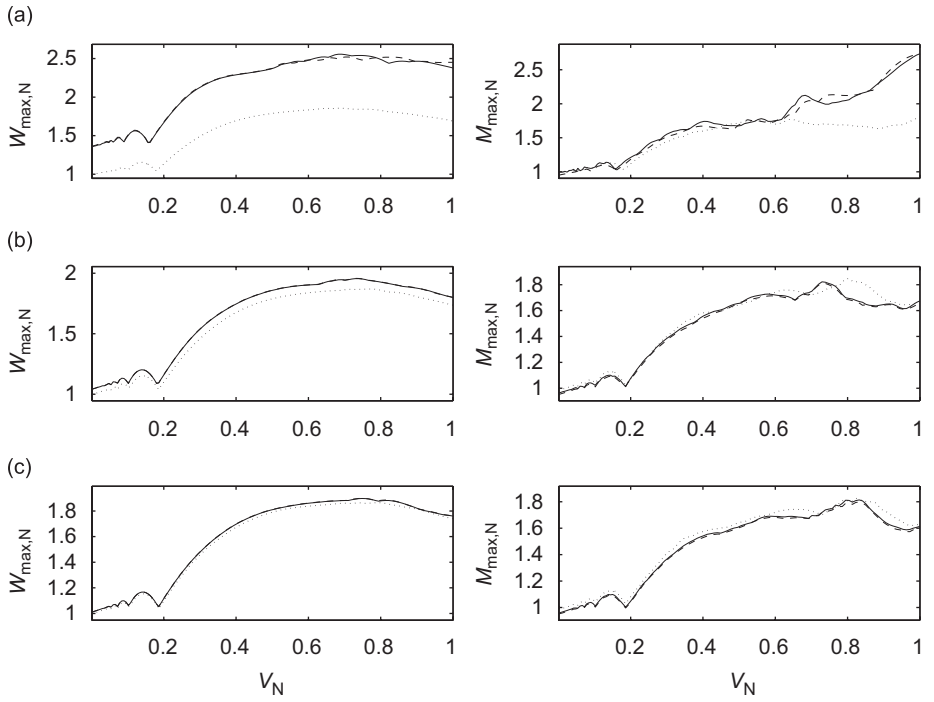

Fig. 7. Effect of the moving mass velocity on the maximum deflection and bending moment of an SS beam for various values of the slenderness parameter: (a) $\lambda = 10$; (b) $\lambda = 30$; (c) $\lambda = 60$ ((···) EBT, (−−) TBT, (—) HOBT; $M_N = 0.15$).

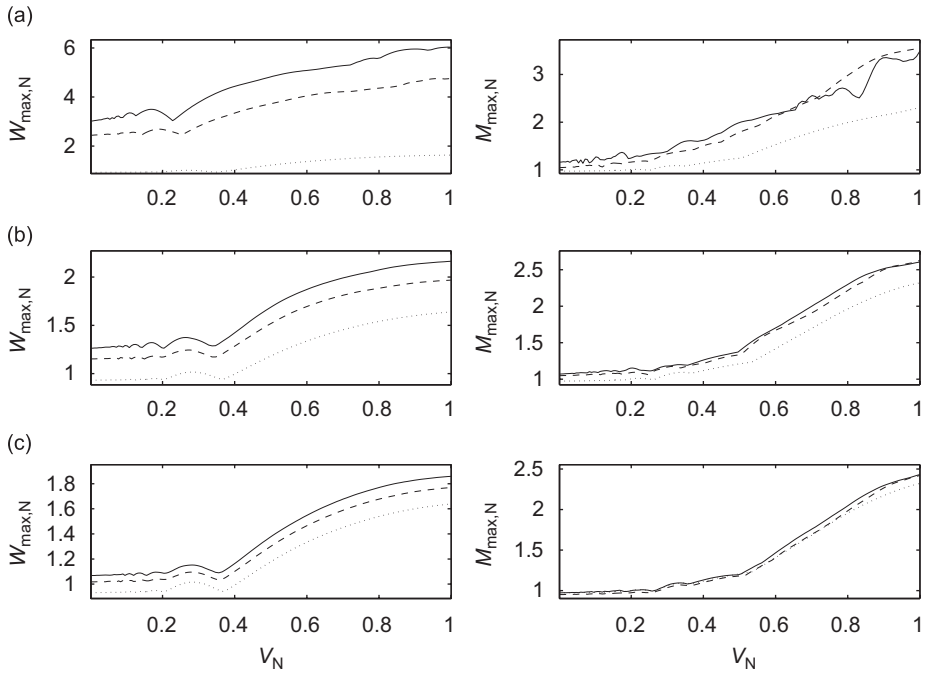

Fig. 8. Effect of the moving mass velocity on the maximum deflection and bending moment of a CC beam for various values of the slenderness parameter: (a) $\lambda = 10$; (b) $\lambda = 30$; (c) $\lambda = 60$ ((···) EBT, (−−) TBT, (—) HOBT; $M_N = 0.15$).

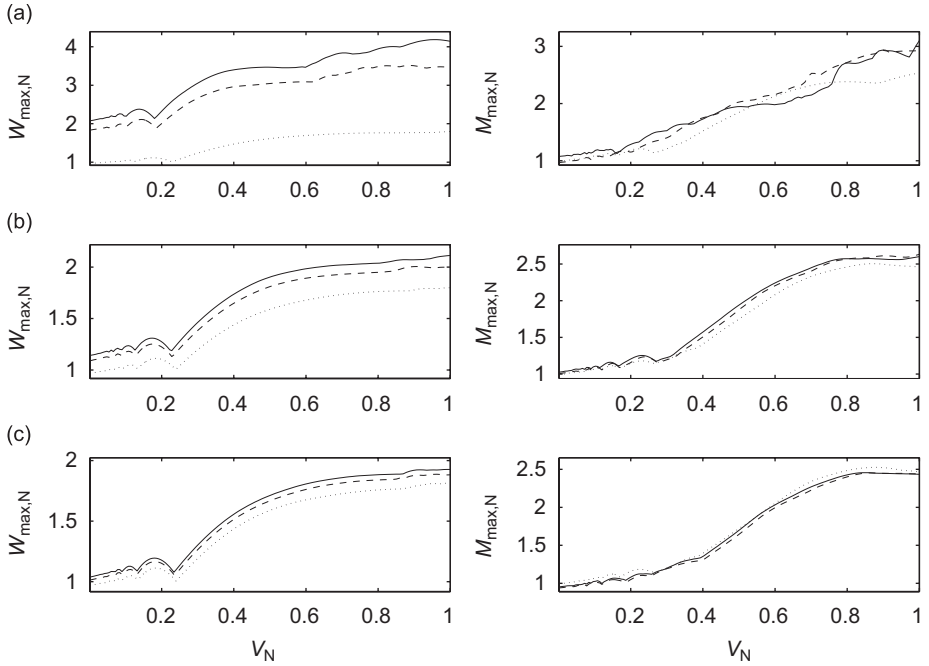

Fig. 9. Effect of the moving mass velocity on the maximum deflection and bending moment of an SC beam for various values of the slenderness parameter: (a) $\lambda = 10$; (b) $\lambda = 30$; (c) $\lambda = 60$ ((···) EBT, (––) TBT, (—) HOBT; $M_N = 0.15$).

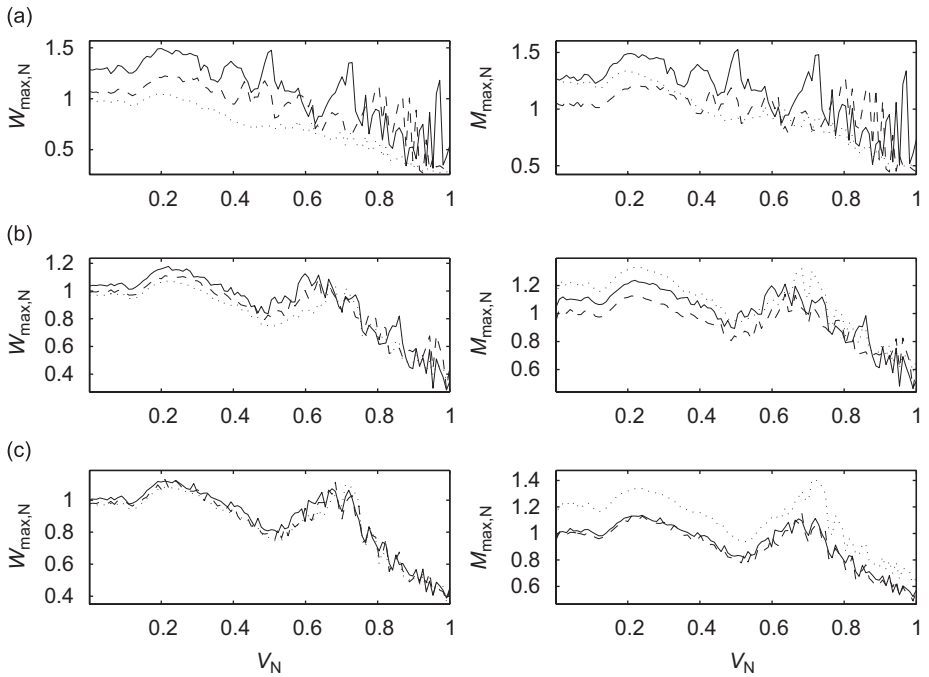

Fig. 10. Effect of the moving mass velocity on the maximum deflection and bending moment of a CF beam for various values of the slenderness parameter: (a) $\lambda = 10$; (b) $\lambda = 30$; (c) $\lambda = 60$ ((···) EBT, (––) TBT, (—) HOBT; $M_N = 0.15$).

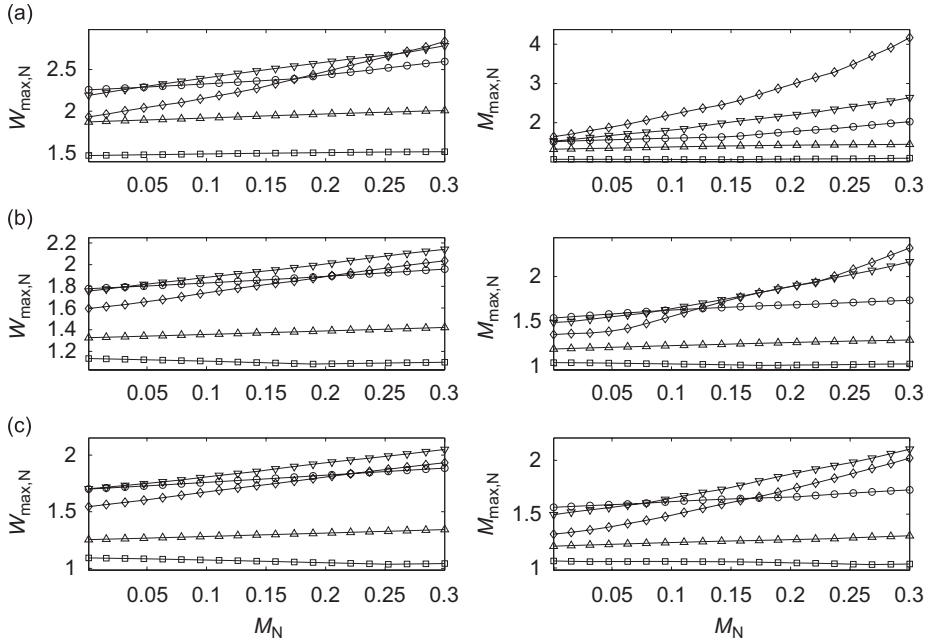

Fig. 11. Effect of mass weight of the moving mass on the maximum deflection and bending moment of an SS beam for various values of the beam slenderness parameter: (a) $\lambda = 10$, analyzed for HOB; (b) $\lambda = 30$, analyzed for TB; (c) $\lambda = 120$, analyzed for EB ((□)$V_N = 0.1$, (Δ)$V_N = 0.25$, (○)$V_N = 0.50$, (∇)$V_N = 0.75$, (◇)$V_N = 1.0$).

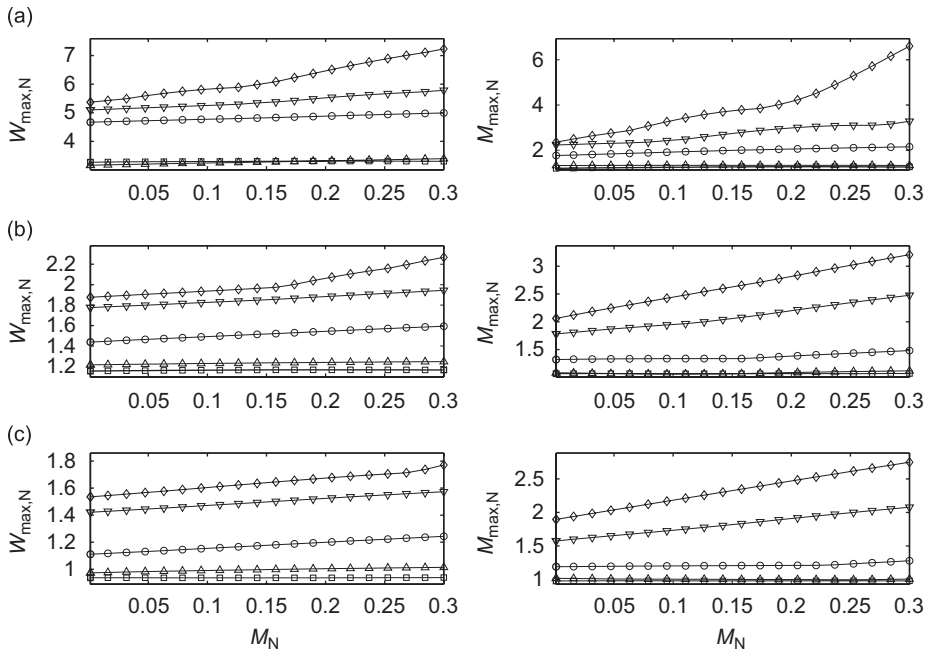

Fig. 12. Effect of mass weight of the moving mass on the maximum deflection and bending moment of a CC beam for various values of the beam slenderness parameter: (a) $\lambda = 10$, analyzed for HOB; (b) $\lambda = 30$, analyzed for TB; (c) $\lambda = 120$, analyzed for EB ((□)$V_N = 0.1$, (Δ)$V_N = 0.25$, (○)$V_N = 0.50$, (∇)$V_N = 0.75$, (◇)$V_N = 1.0$).

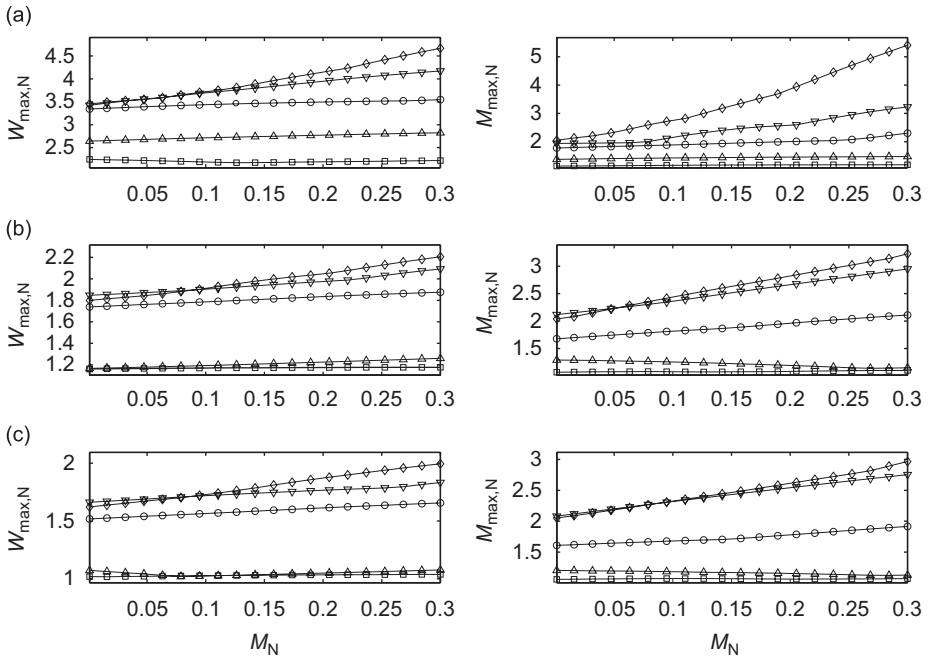

Fig. 13. Effect of mass weight of the moving mass on the maximum deflection and bending moment of an SC beam for various values of the beam slenderness parameter: (a) $\lambda = 10$, analyzed for HOB; (b) $\lambda = 30$, analyzed for TB; (c) $\lambda = 120$, analyzed for EB ($(\square)V_N = 0.1$, $(\Delta)V_N = 0.25$, $(\circ)V_N = 0.50$, $(\nabla)V_N = 0.75$, $(\diamond)V_N = 1.0$).

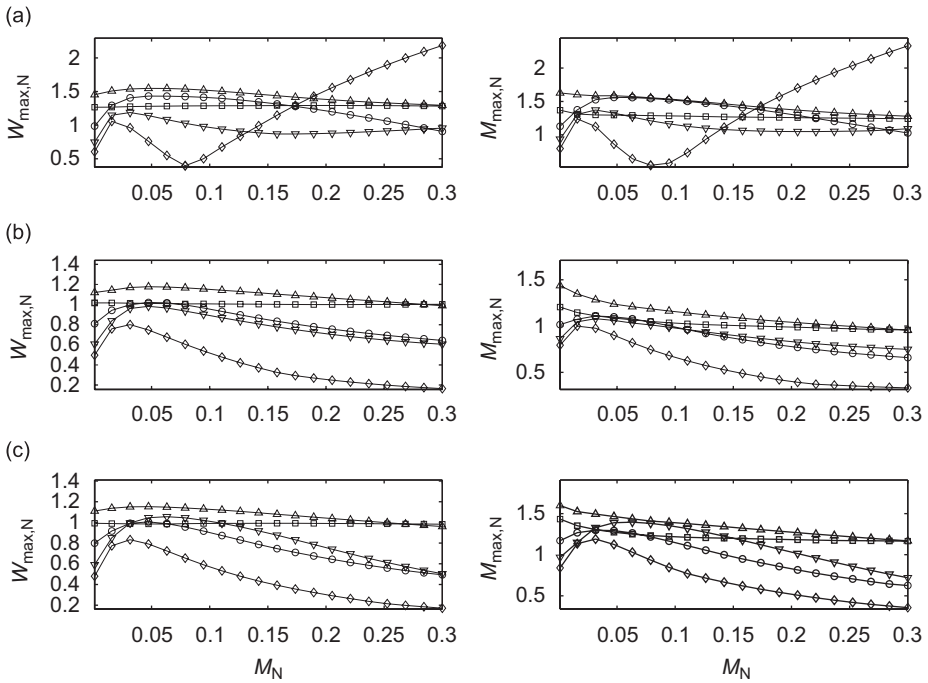

Fig. 14. Effect of mass weight of the moving mass on the maximum deflection and bending moment of a CF beam for various values of beam slenderness parameter: (a) $\lambda = 10$, analyzed for HOB; (b) $\lambda = 30$, analyzed for TB; (c) $\lambda = 120$, analyzed for EB ($(\square)V_N = 0.1$, $(\Delta)V_N = 0.25$, $(\circ)V_N = 0.50$, $(\nabla)V_N = 0.75$, $(\diamond)V_N = 1.0$).

Excluding the cantilever beam (see Fig. 14), there exists a roughly linear relation between the mass weight of the moving load and design parameters of the beam for different velocities of the moving mass. Except for the case of low moving mass velocities ($V_N < 0.25$), in which the slope of the mentioned lines is almost zero, for higher moving mass velocities, any increase in the mass weight of the moving load would lead to linearly proportional higher design parameter values. These results are in complete agreement with those obtained by Nikkhoo et al. [10] for an SS beam. By considering a moderately deeper beam as the slenderness parameter is assumed to be 30, the same parametric study is done but at this slenderness the TBT is used for a proper approach. The results are shown in Figs. 11(b)–14(b) which are completely in line with the aspects of Figs. 11(c)–14(c). Finally, for the case of a very deep beam ($\lambda = 10$), the HOBT is employed to perform a similar parametric study (Figs. 11(a)–14(a)). As Figs. 11(a)–14(a) show, even in very deep beams, the same linear relationis seen clearly for all moving mass velocities. Disparate results in the case of cantilever beam, as shown in Fig. 14, are because of the fact that the maximum responses of the beam occur mostly in the second phase of excitation in which the mass leaves the beam end.

6. Conclusions

Discrete governing equations of motion for Euler–Bernoulli, Timoshenko and higher-order shear beams subjected to a moving mass were developed based on Hamilton's principle. Spatial discretization is done by employing RKPM and the extended Newmark-β method for appropriate time domain discretization. The effects of important parameters such as slenderness and boundary conditions of the beams besides the changes in the magnitude of moving mass weight and velocity have been investigated for various beam theories. In this regard, the design parameter spectra in terms of the beam slenderness, mass weight and velocity of the moving mass were introduced for the mentioned beam theories as well as various boundary conditions. The results indicate that based on the beam boundary condition, there would be a critical beam slenderness in which for slenderness lower than this so-called critical one, EBT or even TBT does not precisely predict the design parameters of the beam under a moving mass. Except for the cantilever beam, the results are indicature of an almost linear relation between the mass weight of the moving mass and the design parameters of the beam for a certain velocity of the moving mass. This is seen for all beam slenderness where the appropriate beam theory is selected. The authors believe that evaluation of crucial design parameters in single-span or multi-span beam structures excited by a distributed moving mass or any other moving systems would be considered as important directions for future works. These studies may give useful guidelines for an optimal structural design for practical applications.

References

[1] M.M. Stanisic, J.C. Hardin, On the response of beam to an arbitrary number of concentrated masses, *Journal of Franklin Institute* 287 (1969) 115–123.
[2] M.M. Stanisic, On a new theory of the dynamic behavior of the structures carrying moving masses, *Ingenieur Archiv* 55 (1985) 176–185.
[3] J.A. Gbadeyan, S.T. Oni, Dynamic behaviour of beams and rectangular plates under moving loads, *Journal of Sound and Vibration* 182 (5) (1995) 677–695.
[4] G.V. Rao, Linear dynamics of an elastic beam under moving loads, *Journal of Vibration and Acoustics* 122 (2000) 281–289.
[5] M.R. Shadnam, F. Rahimzadeh Rofooei, B. Mehri, Dynamics of nonlinear plates under moving mass, *Mechanics Research Communications* 28 (2001) 453–461.
[6] M.R. Shadnam, F. Rahimzadeh Rofooei, M. Mofid, B. Mehri, Periodicity in the response of nonlinear plate under moving mass, *Thin-Walled Structures* 40 (2002) 283–295.
[7] L. Frýba, *Vibration of Solids and Structures under Moving Loads*, Thomas Telford, London, 1999.
[8] E.C. Ting, J. Genin, J.H. Ginsberg, A general algorithm for moving mass problems, *Journal of Sound and Vibration* 33 (1) (1974) 49–58.
[9] E. Esmailzadeh, M. Ghorashi, Vibration analysis of beams traversed by uniform partially distributed moving mass, *Journal of Sound and Vibration* 184 (1) (1995) 9–17.
[10] A. Nikkhoo, F.R. Rofooei, M.R. Shadnam, Dynamic behavior and modal control of beams under moving mass, *Journal of Sound and Vibration* 306 (3–5) (2007) 712–724.

[11] U. Lee, Revisiting the moving mass problem: onset of separation between the mass and beam, *Journal of Vibration and Acoustics* 118 (3) (1996) 516–521.
[12] S. Mackertich, Response of a beam to a moving mass, *Journal of the Acoustical Society of America* 92 (3) (1992) 1766–1769.
[13] H.P. Lee, The dynamic response of a Timoshenko beam subjected to a moving mass, *Journal of Sound and Vibration* 198 (2) (1996) 249–256.
[14] A. Yavari, M. Nouri, M. Mofid, Discrete element analysis of dynamic response of Timoshenko beams under moving mass, *Advances in Engineering Software* 33 (2002) 143–153.
[15] P. Lou, G.L. Dai, Q.Y. Zeng, Finite element analysis for a Timoshenko beam subjected to a moving mass, *Proceedings of the Institution of Mechanical Engineers, Part C, Journal of Mechanical Enginnering Science* 220 (5) (2006) 669–678.
[16] W.K. Liu, S. Jun, S. Li, J. Adee, T. Belytschko, Reproducing kernel particle methods for structural dynamics, *International Journal for Numerical Methods in Engineering* 38 (1995) 1655–1679.
[17] W.K. Liu, S. Jun, Y.F. Zhang, Reproducing kernel particle methods, *International Journal for Numerical Methods in Fluids* 38 (1995) 1655–1679.
[18] J.S. Chen, C. Pan, C.T. Wu, Large deformation analysis of rubber based on a reproducing kernel particle method, *Computational Mechanics* 19 (1997) 211–227.
[19] W.B. Bickford, A constant higher order beam theory, *Development in Theoretical and Applied Mechanics* 11 (1982) 137–142.
[20] P.R. Heyliger, J.N. Reddy, A higher order beam finite element for bending and vibration problems, *Journal of Sound and Vibration* 126 (1988) 309–326.
[21] J.N. Reddy, *Mechanics of Laminated Composite Plates*, CRC Press, Boca Raton, FL, 1997.
[22] A.K. Chopra, *Dynamices of Structures: Theory and Applications to Earthquake Engineering*, third ed., Prentice-Hall, Englewood, Cliffs, NJ, 2001.